

# Evidence for a very low-lying $S = 9$ excited state of the $S = 10$ single molecule magnet $\text{Mn}_{12}$ -acetate

R. S. Edwards,<sup>1</sup> S. Hill,<sup>1,\*</sup> S. Maccagnano,<sup>1</sup> N. S. Dalal,<sup>2</sup> and J. M. North<sup>2</sup>

<sup>1</sup>*Department of Physics, University of Florida, Gainesville, FL 32611, USA*

<sup>2</sup>*Department of Chemistry and National High Magnetic Field Laboratory, Tallahassee, FL 32310, USA*

(Dated: November 20, 2018)

We present a detailed investigation of the temperature and frequency dependence of the anomalous EPR transitions first observed in  $\text{Mn}_{12}$ -acetate by Hill *et al.* [Phys. Rev. Lett. **80**, 2453 (1998)]. The most dominant of these transitions manifest themselves as an extra series of EPR absorption peaks for spectra obtained with the DC field applied within the hard magnetic plane of a single crystal sample. Recent studies by Amigo *et al.* [Phys. Rev. B **65**, 172403 (2002)] have attributed these extra peaks to a strain induced transverse quadratic anisotropy which gives rise to distinct  $\text{Mn}_{12}$ -acetate species, each having a distinct EPR spectrum; on the basis of these measurements, it has been suggested that this transverse anisotropy is responsible for the tunneling in  $\text{Mn}_{12}$ -acetate. Our temperature and frequency dependent measurements demonstrate unambiguously that these anomalous EPR absorptions vanish as the temperature tends to zero, thereby indicating that they correspond to transitions from an excited state of the molecule. We argue that this low lying excited state corresponds to an  $S = 9$  multiplet having very similar zero-field crystal parameters to the  $S = 10$  state, and lying only about  $10 - 15 k_B$  above the  $S = 10$  ( $M_S = \pm 9$ ) ground state. These findings also compare favorably with available neutron scattering data.

PACS numbers: 75.50.Xx, 75.60.Jk, 75.75.+a, 76.30.-v

## I. Introduction

Since it was first suggested that macroscopic quantum tunneling of magnetic moments from one easy axis to another should be observable in ensembles of sufficiently tiny magnetic particles,<sup>1</sup> the quantum properties of crystals containing identical magnetic molecules with relatively large magnetic moments (so far up to  $26\mu_B$ ) – so called single molecule magnets (SMMs)<sup>2,3</sup> – have become the subject of intense research activity. The main feature of magnetic quantum tunneling (MQT) is the following: below a characteristic temperature, called the blocking temperature  $T_B$ , the magnetic viscosity (relaxation time for magnetization reversal) stays finite and temperature independent, indicating that the moments are able to short-circuit the classical thermally activated relaxation channel.<sup>1,2,3,4</sup> SMMs offer a number of advantages over other types of magnetic nanostructures. Most importantly, they are monodisperse. Consequently, they enable fundamental studies of properties intrinsic to magnetic nanostructures that have previously been inaccessible. For example, the observation of well defined quantum jumps in the low temperature ( $T < T_B$ ) hysteresis loops of  $[\text{Mn}_{12}\text{O}_{12}(\text{CH}_3\text{COO})_{16}(\text{H}_2\text{O})_4] \cdot 2\text{CH}_3\text{COOH} \cdot 4\text{H}_2\text{O}$  ( $\text{Mn}_{12}$ -ac) crystals provided evidence for resonant MQT.<sup>2,3,4,5,6</sup> Since this discovery,  $\text{Mn}_{12}$ -ac has become the most widely studied SMM.<sup>2,3,4,5,6,7,8,9,10,11,12,13,14,15,16</sup> The resonant nature of the MQT has enabled very precise studies of the relaxation dynamics,<sup>7,8</sup> while neutron<sup>9,16</sup> and electron paramagnetic resonance (EPR)<sup>10,11,12,13,14,15</sup> experiments have provided fairly detailed spectroscopic information concerning the low-lying quantum energy levels of  $\text{Mn}_{12}$ -ac. In spite of these extensive inves-

tigations, the precise mechanism responsible for the tunneling has remained elusive. An in-depth understanding of MQT is important not only from a fundamental point of view: for example, there has recently been considerable speculation concerning the possible use of SMMs for quantum information processing.<sup>17</sup>

The  $\text{Mn}_{12}$ -ac molecule consists of four  $\text{Mn}^{4+}$  ions, each with spin  $S = \frac{3}{2}$ , surrounded by eight  $\text{Mn}^{3+}$  ions with spin  $S = 2$ .<sup>2,3</sup> The clusters crystallize into a tetragonal lattice, with each molecule having approximate  $S_4$  site symmetry; the orbital moment is quenched, and a Jahn-Teller distortion produces a strong axial anisotropy. A simplified treatment of the magnetic interactions within the molecule has been developed<sup>18</sup> wherein four strongly antiferromagnetically coupled  $\text{Mn}^{3+}$ – $\text{Mn}^{4+}$  dimers, each with spin  $S = 2 - \frac{3}{2} = \frac{1}{2}$ , couple via an effective ferromagnetic interaction to the remaining four  $S = 2$   $\text{Mn}^{3+}$  ions, giving a total spin  $S = 10$ . Within this simplified 8-spin scheme, the weaker couplings between the four spin- $\frac{1}{2}$  dimers and the four spin-2  $\text{Mn}^{3+}$  ions largely determine the low energy excitations within the molecule.<sup>19</sup>

To lowest order, the magnetic energy levels of a rigid spin  $S = 10$  system can be described by the effective spin Hamiltonian:

$$\hat{H} = D\hat{S}_z^2 + \mu_B \vec{B} \cdot \vec{g} \cdot \hat{S} + \hat{H}', \quad (1)$$

where  $D$  ( $< 0$ ) is the uniaxial anisotropy constant, the second term represents the Zeeman interaction with an applied field  $\vec{B}$  ( $\vec{g}$  is the Landé  $g$  tensor), and  $\hat{H}'$  includes higher order terms in the crystal field ( $\hat{O}_4^0, \hat{O}_2^2, \hat{O}_4^2, \hat{O}_4^4$ , etc.<sup>9,10,11,16</sup>), as well as environmental couplings such as intermolecular dipolar and exchange interactions.<sup>12,13,14</sup>

This predominantly Ising-type anisotropy is responsible for the energy barrier to magnetization reversal and the resulting magnetic bistability - factors which lead to magnetic hysteresis at sufficiently low temperatures.<sup>2,3,4</sup> MQT in zero-field is caused by interactions in  $\hat{H}'$  which lower the symmetry of the molecule from strictly axial, thereby mixing otherwise degenerate pure "spin-up" and "spin-down" states. Tunnel rates depend on the degree of symmetry breaking, which is something which can be determined very precisely via single crystal EPR measurements.<sup>10,11,12,13,14,15</sup> The only transverse crystal field term (to fourth order) in  $\hat{H}'$  allowed by the strict  $S_4$  symmetry of the molecule is  $\hat{O}_4^4$ . While such an interaction clearly exists,<sup>10,15,16</sup> it cannot account for many aspects of the low temperature magnetic relaxation.<sup>8,20</sup> For this reason, recent theoretical and experimental attention has focused on a quadratic transverse anisotropy induced by disorder.<sup>8,12,13,14,15,21,22,23,24,25,26</sup> One particular proposal considers long range strains caused by dislocations.<sup>21,22</sup> However, a more likely scenario involves acetate ligand disorder which would give rise to distinct  $\text{Mn}_{12}\text{-ac}$  variants with local site-symmetry lower than  $S_4$ .<sup>8,12,15,26</sup> Indeed, our recent angle dependent EPR studies show clear evidence for a quadratic anisotropy ( $\hat{O}_4^2$ ) which can be attributed to a discrete disorder associated with the ligand molecules.<sup>15</sup> Furthermore, recent magnetic measurements have shown that a narrow distribution of tunnel splittings exists,<sup>8</sup> a fact which is again consistent with the ligand disorder scenario.<sup>26</sup>

In spite of growing acceptance for the role of disorder in the MQT phenomenon, several outstanding questions remain; not least, the absence of a clear parity effect associated with the resonant MQT steps observed in hysteresis experiments.<sup>20</sup> Meanwhile, several recent works have drawn attention to possible inadequacies of the single spin ( $S = 10$ ) description of  $\text{Mn}_{12}\text{-ac}$ .<sup>9,19,27,28,29</sup> For example: a low lying magnetic excitation has been observed in neutron scattering experiments, which cannot be explained within the single spin picture;<sup>9</sup> NMR experiments have demonstrated that the paramagnetic spin density is delocalized over the entire molecule;<sup>27,29</sup> and recent calculations<sup>19</sup> have shown that interactions between the  $S = 10$  multiplet and low lying excited multiplets ( $S < 10$ ) are necessary in order to explain the significant quartic terms in Eq. (1) which are found for  $\text{Mn}_{12}\text{-ac}$ .<sup>10,15,16</sup> In this paper, we present high-frequency single crystal EPR data which provide convincing evidence for a low-lying  $S = 9$  state. We compare these findings with available neutron scattering data,<sup>9</sup> and comment on the possible consequences of these findings.

## II. Experimental

The  $(2S + 1)$ -fold quantum energy level structure associated with a large molecular spin necessitates spectroscopies spanning a wide frequency range. Furthermore, large zero-field level splittings, due to the significant crystalline anisotropy (large  $D$ ) and large total spin  $S$ , demand the use of frequencies and magnetic fields consid-

erably higher (50 GHz to 1 THz, and up to 10 tesla respectively) than those typically used by the majority of EPR spectroscopists. The high degree of sensitivity required for single crystal measurements is achieved using a resonant cavity perturbation technique in combination with a broad-band Millimeter-wave Vector Network Analyzer (MVNA) exhibiting an exceptionally good signal-to-noise ratio; a detailed description of this instrumentation can be found in ref. [30]. The MVNA is a phase sensitive, fully sweepable (8 to 350 GHz), superheterodyne source/detection system. Several sample probes couple the network analyzer to a range of high sensitivity cavities ( $Q$ -factors of up to 25,000) situated within the bore of a superconducting magnet. The MVNA/cavity combination has been shown to exhibit a sensitivity of at least  $10^9$  spins-G<sup>-1</sup>·s<sup>-1</sup>, which is comparable with the best narrow-band EPR spectrometers. This, coupled with newly acquired sources and a split-pair magnet, allow single crystal measurements at any frequency in the range from 8 to 250 GHz, at temperatures down to 1.2 K ( $\pm 0.01$  K), and for any geometrical combination of DC and AC field orientations.

The advantages of a narrow band cavity perturbation technique, and the ability to study single crystals, have recently been discussed in ref. [12]. In particular, such a scheme enables faithful extraction of the intrinsic EPR lineshapes (both the real and imaginary components), free from instrumental artifacts. Consequently, any raw data displayed in this paper constitutes pure absorption. Single  $\text{Mn}_{12}\text{-ac}$  crystals were grown using literature methods.<sup>31</sup> All measurements were performed in the standard EPR configuration with the AC excitation field transverse to the DC field. The two samples (A and B) used in this study were needle shaped, having approximate dimensions  $1 \times 0.1 \times 0.1$  mm<sup>3</sup>. Orientation of the crystals was relatively straightforward due to the shape of the samples, with the needle axis defining the easy axis. All of the presented data were obtained with the DC magnetic field aligned within the samples' hard magnetic ( $x, y$ ) plane (easy axis data are presented in ref. [12]). Low field data ( $< 7$  T) were obtained using a superconducting solenoid, while higher field data were obtained in the resistive magnets at the National High Magnetic Field Laboratory (NHMFL).

## III. Background

In our earlier single crystal investigations of  $\text{Mn}_{12}\text{-ac}$ , we first pointed out that EPR spectra obtained with the field perpendicular to the easy-axis revealed a number of anomalous EPR transitions;<sup>11</sup> these transitions were labeled  $\beta$  and  $\gamma$  in ref. [11], as opposed to the  $\alpha$ -resonances which nicely fit the accepted  $S = 10$  Hamiltonian for  $\text{Mn}_{12}\text{-ac}$  (see Fig. 1 and Table 1, which adopts this same labeling scheme). These earlier studies were conducted at moderate fields ( $B < 11$  T), and at relatively low frequencies compared to the powder studies by Barra *et al.*<sup>10</sup> In the high-field limit, one expects 20 transitions within the  $2S + 1$  ( $S = 10$ ) multiplet; the  $\alpha$ -resonances in ref. [11]

and Fig. 1 comprise half of this total (corresponding to transitions from  $M_S = \text{even-to-odd}$  integers, see Table 1). One should eventually expect to see an additional 10 EPR peaks, in between the  $\alpha$ -resonances (corresponding to transitions from  $M_S = \text{odd-to-even}$  integers), but only in the high-field/frequency limit; Fig. 2 illustrates the origin of these transitions. We previously tentatively ascribed the  $\beta$ -resonances to the expected high-field resonances. However, the  $M_S = \text{odd-to-even}$  transitions should become EPR silent below about 95 GHz (due to avoided level crossings, see Fig. 2b), yet they persist down to at least 45 GHz. Indeed, all attempts to fit the  $\beta$ -resonances to the accepted  $\text{Mn}_{12}$ -ac Hamiltonian (Eq. 1) have failed quite spectacularly. We should point out that we have since carried out single crystal studies on simpler  $S = \frac{9}{2}$   $\text{Mn}_4$  SMMs (corresponding to the core of the  $\text{Mn}_{12}$  SMM), with the same  $S_4$  symmetry, which behave absolutely as expected according to Eq. 1.<sup>32</sup>

More recently, several other groups have reported extra EPR peaks for both single crystal studies with the field perpendicular to the easy axis, and from powder measurements. Amigo *et al.*<sup>23</sup> ascribe the extra peaks to a strain or disorder induced transverse anisotropy (caused by dislocations in the sample, see ref. [21,22]), which gives rise to different species of molecule within the crystal. In this model, the extra peaks arise due to the fact that one expects equal numbers of molecules having their hard axes along a particular direction in the hard plane, and at  $90^\circ$  to this direction. Matters are complicated further due to the fact that their model includes a rather broad distribution of transverse anisotropies. Thus, it is unlikely that one would observe distinct splittings in such a case, but rather a broadening of the resonance linewidths, with an EPR lineshape that reflects the distribution. Cornia *et al.* have also recently published data which show a splitting of the  $\alpha$ -resonances (the  $\beta$  resonances are also seen in their 95 GHz spectra).<sup>26</sup> However, this splitting is more subtle, since it is only clearly observed using field modulation, or by taking derivatives of absorption spectra.<sup>15</sup> We also see this effect in the  $\alpha$ -resonances (this is the subject of a separate publication<sup>15</sup>). Cornia *et al.* propose a mechanism for this splitting involving disorder associated with the acetic acids of crystallization. Like Amigo's model, this ligand disorder induces a transverse anisotropy which varies from one molecule to the next.

We believe that the EPR splittings observed by Amigo *et al.*,<sup>23</sup> and by Cornia *et al.*,<sup>26</sup> have quite different origins. The latter almost certainly are associated with ligand disorder, as we have recently confirmed,<sup>15</sup> whereas the distinct absorptions observed by Amigo *et al.* correspond to the same  $\beta$ -resonances that we observed in our original single crystal investigations.<sup>11</sup> Although Amigo *et al.* claim that the anomalous peaks are only observed upon stressing their samples, there is clear evidence for such resonances even in their unstressed samples (see Fig. 2 in ref. [23]). Furthermore, we have seen these extra peaks in all of the samples that we have studied, as

have Barra *et al.*<sup>10</sup> and Cornia *et al.*<sup>26</sup> There do, however, appear to be noticeable differences in the positions and intensities of anomalous EPR peaks obtained by different groups. Since transverse EPR spectra are notoriously sensitive to field alignment,<sup>15</sup> minor differences in sample orientation may easily explain these differences, as could solvent loss from the samples.

#### IV. Results and discussion

Figure 1 shows data obtained for sample A at four different frequencies from 44 GHz up to 111 GHz; the temperature is 10 K for each sweep. The dips in absorption are due to EPR transitions, and these have been labeled according to the original scheme in ref. [11]. The  $\alpha$ -resonances correspond to transitions within the Zeeman split energy levels which, in zero-field, correspond to  $M_S = \pm m$  states ( $m = \text{integer}$ , and  $0 \leq m \leq S$ ) as depicted in Fig. 2a; in this representation, the quantization axis is defined by the uniaxial crystal field tensor, and is along  $z$ . In the high-field limit, the quantization axis points along the applied field vector; in this limit, the ten  $\alpha$ -resonances correspond to transitions from  $M_S = \text{even-to-odd } m$ , *e.g.*  $M_S = -10$  to  $-9$  (again, this situation is illustrated in Fig. 2a). Because the  $\alpha$ -resonances originate from pairs of levels which are (approximately) degenerate in zero field, one expects the resonance frequencies, when plotted against field, to tend to zero as the field tends to zero; this can be seen in Fig. 2b.

In the high field limit, one expects ten additional resonances corresponding to  $M_S = \text{odd-to-even } m$ , *e.g.*  $M_S = -9$  to  $-8$ . Indeed, we do see these transitions at high fields (see below). However, if one follows these transitions to the zero-field limit, it is clear that the resonance frequency should go through a minimum, tending to one of the zero-field splittings in this limit; this is illustrated in Fig. 2a and by the dashed curves in Fig. 2b. Consequently, such EPR transitions should become "EPR silent" below some characteristic cut-off frequency determined by the point of closest approach for the two levels involved in the transition. The dominant interaction responsible for this level repulsion is simply the Zeeman term in Eq. 1 and is, therefore, more-or-less insensitive to the other transverse terms in Eq. 1. For  $\text{Mn}_{12}$ -ac, this cut-off frequency is about 95 GHz for the three highest field odd-to-even  $m$  transitions (see Fig. 2b, which uses realistic parameters for  $\text{Mn}_{12}$ -ac).<sup>15,16</sup> For this reason, below 95 GHz, the  $\beta$ -resonances observed in Fig. 1 cannot be attributed to the high-field odd-to-even  $m$  transitions. However, it is noticeable that the strength of the  $\beta$ -resonances increases dramatically between the 77.4 GHz trace and the 111.1 GHz trace, *i.e.* above 95 GHz, there is a pronounced increase in the strength of the  $\beta$ -resonance. We shall comment more on this below.

Next, we turn to the temperature dependence of the data obtained in Fig. 1, with particular attention being paid to the highest field  $\beta$ -resonance ( $\beta_{10}$ ), and a much weaker  $\gamma$ -resonance. Fig. 3 shows data for three frequencies below the cut-off of 95 GHz. In all of these traces,

the  $\beta 10$  resonance diminishes in intensity as  $T \rightarrow 0$ , becoming more-or-less invisible at the lowest temperature. This fact proves beyond any doubt that the  $\beta 10$  resonance originates from an excited state of the  $\text{Mn}_{12}\text{-ac}$  molecule, thereby ruling out any likelihood that it corresponds to a different  $\text{Mn}_{12}\text{-ac}$  species, as proposed by Amigo *et al.*<sup>23</sup> We will discuss the possible origin of this excited state further below. Meanwhile, we note that the weak  $\gamma$ -resonance exhibits a very similar temperature dependence to the  $\alpha 10$  resonance, which corresponds to the transition from the accepted  $S = 10$  ground state of the molecule, *i.e.* the  $\gamma$  and  $\alpha 10$  peaks continue to grow as  $T \rightarrow 0$ . Therefore, there is every likelihood that the  $\gamma$  peak does signify a small minority ( $\sim 1$  to  $2\%$ ) of molecules having a different ground state from the majority. We speculate that this peak may correspond to the well known faster relaxing species of  $\text{Mn}_{12}\text{-ac}$ , which has one of its Jahn-Teller axes tilted with respect to the  $z$ -axis of the molecule.<sup>33,34</sup> This peak has only been observed for some samples, a fact which is also consistent with the faster relaxing species. The faster relaxing  $\text{Mn}_{12}\text{-ac}$  Jahn-Teller isomer is believed to have an  $S = 9$  ground state, a reduced axial anisotropy constant ( $D$ -value) and an appreciable transverse quadratic anisotropy.<sup>35</sup> All of these factors can explain the fact that the  $\gamma$ -resonance is observed at lower fields than the  $\alpha 10$  resonance. However, the shift appears to be rather large, implying a  $\sim 30\%$  reduction in  $D$  over the majority species; further studies on pure samples of the faster relaxing species are planned in the near future in order to resolve this issue. A similar weak lower lying peak has been observed in neutron scattering experiments where, again, the authors attribute this to the faster relaxing  $\text{Mn}_{12}\text{-ac}$  species.<sup>16</sup> It is interesting to note that the ratios of the frequencies of the presumed fast and slow relaxing peaks observed here, and from neutron scattering are quite similar,<sup>16</sup> as are the relative intensities.

Figure 4 shows the temperature dependence of the 111.1 GHz data from Fig. 2. At this frequency, which is above the cut-off for odd-to-even  $m$  high-field transitions, the  $\beta 10$  resonance shows a marked increase in intensity over the lower frequency data. Indeed, it exceeds the intensity of the  $\alpha 10$  resonance at temperatures above about 4.2 K. Furthermore,  $\beta 10$  is clearly visible at the lowest temperatures investigated. A similar trend may be noted for  $\beta 9$ . We suspect that this pronounced enhancement of  $\beta 10$  (and  $\beta 9$ ) is caused by the switching on of the anticipated high-field  $M_S = -9$  to  $-8$  ( $-7$  to  $-6$ ) transition within the  $S = 10$  state of  $\text{Mn}_{12}\text{-ac}$  (see Fig. 2 and Table 1); the fact that it is difficult to distinguish these transitions from the anomalous low frequency transitions will be discussed further below. EPR spectra obtained with the field applied parallel to the easy ( $z$ -) axis show no additional anomalous peaks,<sup>12</sup> *i.e.* no EPR absorptions which cannot be explained within the framework of the  $S = 10$  picture. Easy axis data obtained over a wider frequency range (40 to 200 GHz) compared to our earlier studies (ref. [11]) have recently been published in

ref. [12].

Recent hard axis measurements for a second sample (B), covering a wider frequency range compared to our original investigations,<sup>11</sup> have enabled a complete determination of the Hamiltonian parameters for  $\text{Mn}_{12}\text{-ac}$  up to fourth order.<sup>15</sup> Further details of our fitting procedure are published elsewhere.<sup>15</sup> Fig. 5 shows the results of such a fit, along with the obtained parameters. As can be seen, the solid curves ( $S = 10$  picture) lie beautifully on the  $\alpha$ -resonance data (open circles). However, as already discussed, the  $\beta$ -resonances (solid squares) only match the  $S = 10$  curves at the highest frequencies investigated; below 95 GHz, a dramatic departure from the expected behavior can be seen. It is impossible to force the  $S = 10$  fits through these low frequency  $\beta$ -resonance data points, since it is apparent that they belong to curves which approach zero frequency as the field tends to zero; for an  $S = 10$  system, the high-field odd-to-even  $m$  transitions tend to finite frequency offsets in the low field limit (see Fig. 2). We therefore speculate that, at low frequencies, the  $\beta$ -resonances correspond to transitions within an excited state of  $\text{Mn}_{12}\text{-ac}$ . For comparison, Fig. 5 includes curves corresponding to the  $S = 9$  state, which were generated using precisely the same parameters as obtained from the  $S = 10$  fit. For an odd total spin state, the low field limiting behavior of odd-to-even  $m$  and even-to-odd  $m$  transitions is the reverse of that for an even total spin state. Consequently, one *does expect* the frequency of the  $M_S = -9$  to  $-8$  transition to go to zero in the low field limit for  $S = 9$ . Although not perfect, the low frequency  $\beta$ -resonance data lie quite close to the  $S = 9$  curves. At higher frequencies, the  $\beta$ -resonances lie somewhat in between the  $S = 9$  and  $S = 10$  curves while, in the high frequency limit, they lie nicely on the  $S = 10$  curves.

Having noted the possible connection between the  $\beta$ -resonances and an  $S = 9$  state, one has to ask whether such an assignment is consistent with other published results. Based on the limited temperature dependence of  $\beta 10$  (Fig. 3), we can estimate the approximate activation energy to the state from which  $\beta 10$  is excited, *i.e.* the presumed  $S = 9$  state. This analysis is complicated somewhat by the broad asymmetric  $\alpha 10$  resonance, and due to the fact that the  $\beta 10$  resonance saturates at temperatures as low as 4–6 K. Nevertheless, a crude analysis yields a very low activation energy of 10–15  $k_B$ . Incredibly, this implies that the supposed  $S = 9$  ( $M_S = \pm 9$ ) state lies very close to the first excited state of the  $S = 10$  multiplet! Even looking by eye at the data in Fig. 3, one can see that the temperature dependence of  $\beta 10$  and  $\alpha 9$  are quite similar, so it is clear that the activation energy to the  $S = 9$  state is of a similar order to the low lying  $S = 10$  levels. An energy of 10  $k_B$  corresponds precisely to 0.2 THz, where a very strong finite  $Q$  ( $1.18 \text{ \AA}^{-1}$ ) mode has been observed from neutron scattering experiments.<sup>9</sup> The momentum dependence of the intensity of this mode indicates that it has a magnetic origin (its intensity tends to zero as  $Q \rightarrow 0$ ), suggesting spins that are coupled on a local scale. Indeed, from an analysis of the neutron data,

one can conclude that this mode may be related to the antiferromagnetic coupling within a  $\text{Mn}^{3+}-\text{Mn}^{4+}$  dimer within the framework of the  $\text{Mn}_{12}$  molecule.<sup>9</sup>

Recent theoretical studies of the spin excitations within  $\text{Mn}_{12}$ -ac treat the molecule as a system of four strongly antiferromagnetically coupled  $\text{Mn}^{3+}-\text{Mn}^{4+}$  dimers, each with spin  $S = 2 - \frac{3}{2} = \frac{1}{2}$  which, in the ground state, are coupled via an effective ferromagnetic interaction to the four remaining  $\text{Mn}^{3+}$  ions, each having  $S = 2$ .<sup>18,19,28</sup> Within this simplified scheme, the weaker couplings between the four spin- $\frac{1}{2}$  dimers and the four spin-2  $\text{Mn}^{3+}$  ions largely determine the low energy excitations within the molecule. While these calculations do not reproduce the 0.2 THz neutron mode,<sup>9</sup> this 8 spin model provides a basis for comparison with the present data. In particular, one could imagine an excitation within a spin- $\frac{1}{2}$  dimer leading to a reversal of this moment, and to an overall  $S = 9$  state for the molecule. It was previously speculated that the 0.2 THz mode originates from dissipative interactions between the  $\text{Mn}_{12}$  clusters and their environment.<sup>19</sup> The present work seems to indicate that this is not the case, and that the 0.2 THz mode corresponds to a distinct finite  $Q$  excitation of the molecule to a well defined (probably  $S = 9$ ) state. We hope that these findings will stimulate further theoretical work on this problem.

While our measurements do not provide definitive proof that the low lying excitation within the molecule corresponds to an  $S = 9$  state, such an explanation for the observed trends in the single crystal EPR data is quite appealing. Furthermore, it is apparent that the  $S = 9$  and  $S = 10$  data become indistinguishable in the high frequency limit, which would explain why other researchers have successfully simulated most aspects of their high-field powder EPR data using an  $S = 10$  model.<sup>10,23</sup> A summary of the tentative assignments of the resonances is presented in Table 1. In order to simplify the ensuing discussion, we shall assume that the observed excited state does, in fact, correspond to  $S = 9$ . The fact that the  $\beta$  resonances merge smoothly into the  $S = 10$  model at high frequencies suggests that the parameters describing the  $S = 9$  state of the molecule are quite similar to those describing the  $S = 10$  state. To a first approximation, this is not so unrealistic since this merely corresponds to the reversal of the moment of one of the dimers. Consequently, one would expect excitations within the  $S = 9$  and  $S = 10$  multiplets to be virtually indistinguishable for fields parallel to the easy axis, since there is no distinction between even-to-odd  $m$  and odd-to-even  $m$  transitions for this orientation. This fact, again, appears to be consistent with our experimental findings. Minor mismatches in the parameters could give rise to temperature dependent line shapes and widths. In particular, one could expect some line narrowing upon depopulating the  $S = 9$  state at low temperatures. Such behavior has been observed, and explained very well in terms of inter-molecular dipolar interactions.<sup>12,13,14</sup> Without more precise data for the

$S = 9$  state, it is not possible to say whether this picture needs to be re-evaluated.

Due to the finite momentum separating the  $S = 9$  and  $S = 10$  states, it is clear that there could be no direct evidence for the 0.2 THz excitation from optical studies, *i.e.* no direct optical transitions from the  $S = 10$  ground state, to the low-lying  $S = 9$  state. Indeed, no such transitions ( $\sim 0.2$  THz) have been reported. However, excitations within each manifold ( $S = 10$  and  $S = 9$ ) are allowed, as appears to be the case from these EPR investigations. Furthermore, the finite momentum separation would tend to minimize any interaction between these two states, thereby explaining why the  $S = 10$  picture explains so many low-temperature experimental observations with such precision, including most EPR data. Nevertheless, even very weak interactions between these states could have crucial implications as far as the tunneling is concerned in  $\text{Mn}_{12}$ -ac. Clearly further theoretical studies are required.

## V. Summary and conclusions

Detailed single crystal EPR investigations of  $\text{Mn}_{12}$ -ac reveal several transitions in the hard axis spectra which do not fit the accepted  $S = 10$  picture; indeed, the deviations of these EPR peaks from the  $S = 10$  theory are quite dramatic. Temperature dependent studies indicate that the anomalous transitions originate from an excited state of the molecule which lies only about  $10 - 15 k_B$  above the  $S = 10$ ,  $M_S = \pm 10$  ground state, *i.e.* approximately coincident with the first excited state of the  $S = 10$  multiplet. These observations conflict with the recent suggestion by Amigo *et al.* that the anomalous peaks correspond to unique disorder-induced ground states of  $\text{Mn}_{12}$ -ac.<sup>23</sup>

Independent evidence for a low-lying ( $\sim 10 - 15 k_B$ ) excitation to something other than the standard  $S = 10$  state has been known for some time from neutron scattering experiments.<sup>9</sup> The present EPR investigations show, unambiguously, that this low-lying state is very real; indeed, both studies agree on the activation energy. Based on extensive frequency dependent measurements, we argue that the excited state corresponds to an  $S = 9$  multiplet having very similar zero-field crystal field parameters to the  $S = 10$  state. While our measurements do not provide definitive proof for such an  $S = 9$  state, this assignment would explain why there is little evidence for its existence in most other EPR and optical studies published to date. The effects of this low-lying  $S = 9$  state on the low-temperature quantum properties of  $\text{Mn}_{12}$ -ac are not known, and we hope these investigations will stimulate further theoretical studies.

## VI. Acknowledgements

We thank Andy Kent, George Christou and David Hendrickson for useful discussion. This work was supported by the NSF (DMR0103290, DMR0196430 and DMR0239481); the NHMFL is supported by the State of Florida and the NSF under DMR0084173. S. H. would

like to thank the Research Corporation for financial support.

- 
- \* corresponding author, Email:hill@phys.ufl.edu
- <sup>1</sup> C. P. Bean and J. D. Livingston, J. Appl. Phys. **30**, 120S (1959).
  - <sup>2</sup> G. Christou, D. Gatteschi, D. Hendrickson, and R. Sessoli, MRS Bulletin **25**, 66 (2000).
  - <sup>3</sup> D. Gatteschi and R. Sessoli, Angew. Chem. **42**, 268 (2003).
  - <sup>4</sup> E. M. Chudnovsky and J. Tejada, *Macroscopic Quantum Tunneling of the Magnetic Moment* (Cambridge University Press, Cambridge, 1998).
  - <sup>5</sup> J. R. Friedman, M. P. Sarachik, J. Tejada, and R. Ziolo, Phys. Rev. Lett. **76**, 3830 (1996).
  - <sup>6</sup> L. Thomas, F. Lioni, R. Ballou, D. Gatteschi, R. Sessoli, and B. Barbara, Nature **383**, 145 (1996).
  - <sup>7</sup> J. M. Hernandez, X. X. Zhang, F. Luis, J. Tejada, J. R. Friedman, M. P. Sarachik, and R. Ziolo, Phys. Rev. B **55**, 5858 (1997).
  - <sup>8</sup> E. del Barco, A. D. Kent, E. M. Rumberger, D. N. Hendrickson, and G. Christou, Europhys. Lett. **60**, 768 (2002).
  - <sup>9</sup> M. Hennion, L. Pardi, I. Mirebeau, E. Suard, R. Sessoli, and A. Caneschi, Phys. Rev. B **56**, 8819 (1997).
  - <sup>10</sup> A. L. Barra, D. Gatteschi, and R. Sessoli, Phys. Rev. B **56**, 8192 (1997).
  - <sup>11</sup> S. Hill, J. A. A. J. Perenboom, N. S. Dalal, T. Hathaway, T. Stalcup, and J. S. Brooks, Phys. Rev. Lett. **80**, 2453 (1998).
  - <sup>12</sup> S. Hill, S. Maccagnano, K. Park, R. M. Achey, J. M. North, and N. S. Dalal, Phys. Rev. B **66**, 224410 (2002).
  - <sup>13</sup> K. Park, M. Novotny, N. Dalal, S. Hill, and P. Rikvold, Phys. Rev. B **65**, 14426 (2002).
  - <sup>14</sup> K. Park, M. Novotny, N. Dalal, S. Hill, and P. Rikvold, Phys. Rev. B **66**, 144409 (2002).
  - <sup>15</sup> S. Hill, R. S. Edwards, S. I. Jones, J. M. North, and N. S. Dalal, cond-mat/0301599 (Jan, 2003) (unpublished).
  - <sup>16</sup> I. Mirebeau, M. Hennion, H. Casalta, H. Andres, H. U. Güdel, A. V. Irodova, and A. Caneschi, Phys. Rev. Lett. **83**, 628 (1999).
  - <sup>17</sup> M. N. Leuenberger and D. Loss, Nature **410**, 789 (2001).
  - <sup>18</sup> R. Sessoli, H.-L. Tsai, A. Shake, S. Wang, J. Vincent, K. Folting, D. Gatteschi, G. Christou, and D. Hendrickson, J. Am. Chem. Soc. **115**, 1804 (1993).
  - <sup>19</sup> M. I. Katsnelson, V. V. Dobrovitski, and B. N. Harmon, Phys. Rev. B **59**, 6919 (1999).
  - <sup>20</sup> J. R. Friedman, M. P. Sarachik, and R. Ziolo, Phys. Rev. B **58**, R14729 (1998).
  - <sup>21</sup> E. M. Chudnovsky and D. A. Garanin, Phys. Rev. Lett. **87**, 187203 (2001).
  - <sup>22</sup> D. A. Garanin and E. M. Chudnovsky, Phys. Rev. B **65**, 094423 (2002).
  - <sup>23</sup> R. Amigó, E. del Barco, L. Casas, E. Molins, J. Tejada, I. B. Rutel, B. Mommouton, N. Dalal, and J. Brooks, Phys. Rev. B **65**, 172403 (2002).
  - <sup>24</sup> B. Parks, J. Loomis, E. Rumberger, D. N. Hendrickson, and G. Christou, Phys. Rev. B **64**, 184426 (2001).
  - <sup>25</sup> K. M. Mertes, Y. Suzuki, M. P. Sarachik, Y. Paltiel, H. Shtrikman, E. Zeldov, E. Rumberger, D. N. Hendrickson, and G. Christou, Phys. Rev. Lett. **87**, 227205 (2001).
  - <sup>26</sup> A. Cornia, R. Sessoli, L. Sorace, D. Gatteschi, A. L. Barra, and C. Daugebonne, Phys. Rev. Lett. **89**, 257201 (2002).
  - <sup>27</sup> R. M. Achey, P. L. Kuhns, A. P. Reyes, W. G. Moulton, and N. S. Dalal, Phys. Rev. B **64**, 064420 (2001).
  - <sup>28</sup> S. Yamamoto and T. Nakanishi, Phys. Rev. Lett. **89**, 157603 (2002).
  - <sup>29</sup> R. M. Achey, P. L. Kuhns, A. P. Reyes, W. G. Moulton, and N. S. Dalal, Solid State Commun. **121**, 107 (2002).
  - <sup>30</sup> M. Mola, S. Hill, P. Goy, and M. Gross, Rev. Sci. Instr. **71**, 186 (2000).
  - <sup>31</sup> T. Lis, Acta Cryst. B **36**, 2042 (1990).
  - <sup>32</sup> R. S. Edwards, S. Hill, S. Bhaduri, N. Aliaga-Alcade, E. Bolin, S. Maccagnano, G. Christou, and D. N. Hendrickson (unpublished).
  - <sup>33</sup> Z. Sun, D. Ruiz, N. R. Dilley, M. Soler, J. Ribas, K. Folting, M. B. Maple, G. Christou, and D. N. Hendrickson, Chem. Commun. **1999**, 1973 (1999).
  - <sup>34</sup> S. M. J. Aubin, Z. Sun, H. J. Eppley, E. M. Rumberger, I. A. Guzei, K. Folting, P. K. Gantzel, A. L. Rheingold, G. Christou, and D. N. Hendrickson, Inorg. Chem. **40**, 2127 (2001).
  - <sup>35</sup> G. Christou, private communication (unpublished).

TABLE I: Tentative assignments of the  $\alpha$ - and  $\beta$ -resonances observed in this study, based on the high-field representation in which  $M_S$  represents the spin projection along the applied field axis. HF and LF refer respectively to high- and low-frequency limits.

Resonance	HF/LF	$M_S$	Spin
$\alpha 10$	HF	$-10 \rightarrow -9$	10
$\alpha 9$	HF	$-8 \rightarrow -7$	10
$\alpha 8$	HF	$-6 \rightarrow -5$	10
$\alpha 7$	HF	$-4 \rightarrow -3$	10
$\beta 10$	HF	$-9 \rightarrow -8$	10, 9
$\beta 9$	HF	$-7 \rightarrow -6$	10, 9
$\beta 8$	HF	$-5 \rightarrow -4$	10, 9
$\beta 10$	LF	$-9 \rightarrow -8$	9
$\beta 9$	LF	$-7 \rightarrow -6$	9

## Figure captions

FIG. 1. Frequency dependence of the hard axis EPR spectra for Mn<sub>12</sub>-ac (sample A); the temperature and the frequencies are indicated in the figure. The  $\alpha$ -resonances behave as expected for a spin  $S = 10$  easy axis system. The anomalous  $\beta$ -resonances increase in intensity with increasing frequency, becoming particularly prominent at the highest frequency; these transitions are indicated with dots ( $\beta_{10}$ ) and arrows ( $\beta_9$ ). Assignments of the various resonances are listed in Table 1, and Fig. 2 illustrates the possible spin  $S = 10$  transitions.

FIG. 2. The upper panel shows the energy level diagram for Mn<sub>12</sub>-ac for a field applied within the hard plane; this simulation was made using accepted Hamiltonian parameters for Mn<sub>12</sub>-ac ( $D = -0.454$  cm<sup>-1</sup>,  $B_4^0 = -2.0 \times 10^{-5}$  cm<sup>-1</sup>,  $B_4^4 = \pm 3.0 \times 10^{-5}$  cm<sup>-1</sup>).<sup>15,16</sup> The vertical bars illustrate the origin of the  $\alpha$ -resonances (even-to-odd  $M_S$  transitions), while the filled circles represent the high frequency odd-to-even  $M_S$  transitions. The quantum state labels on the left hand side of the figure correspond to the spin projection along  $z$  (low-field limit), while the labels on the right hand side correspond to the spin projection along the applied field direction (high-field limit). The lower panel plots the expected transition frequencies, as a function of magnetic field, for the transitions labeled in the upper panel. The main point to note is the fact that the odd-to-even  $M_S$  transition frequencies (dashed lines) go through a minimum. Therefore, these transitions should not be observable below a cut-off frequency which is about 95 GHz for the first few resonances in Mn<sub>12</sub>-ac.

FIG. 3. Temperature dependence of the hard axis EPR spectra obtained at three frequencies below the hard axis cut-off frequency (see Fig. 2 for explanation) for sample A; the temperatures and frequencies are indicated in the figure. The main point to note is that only the  $\alpha$ - and  $\gamma$ -resonances persist as  $T \rightarrow 0$ ; the intensities of the  $\beta$ -resonances, on the other hand, go to zero as  $T \rightarrow 0$ . Consequently, only the  $\alpha$ - and  $\gamma$ -peaks can be attributed to ground states of Mn<sub>12</sub>-ac - see main text for further discussion.

FIG. 4. Temperature dependence of the hard axis EPR spectra obtained above the hard axis cut-off frequency (see Fig. 2 for explanation) for sample A; the temperature and the frequencies are indicated in the figure. In contrast to Fig. 3, the  $\beta$ -resonance shows appreciable intensity, even at the lowest temperature while, at the highest temperature, it is by far the strongest peak.

FIG. 5. Fits of the frequency dependence of hard axis spectra obtained for sample B. Details of this analysis are published elsewhere.<sup>15</sup> The  $\alpha$ -resonances (open circles) fit the  $S = 10$  model (solid lines) exceptionally well. The  $\beta$ -resonances (solid squares), on the other hand, only fit

the  $S = 10$  picture at higher frequencies. It is not possible to force the  $S = 10$  fits through the  $\beta$  resonance data points observed below 95 GHz. However, it is found that these low-frequency points lie quite close to the behavior expected for  $S = 9$  (dashed curves). The inset depicts the orientation of the applied field relative to the sample, and the obtained quadratic and quartic Hamiltonian parameters are indicated in the figure.



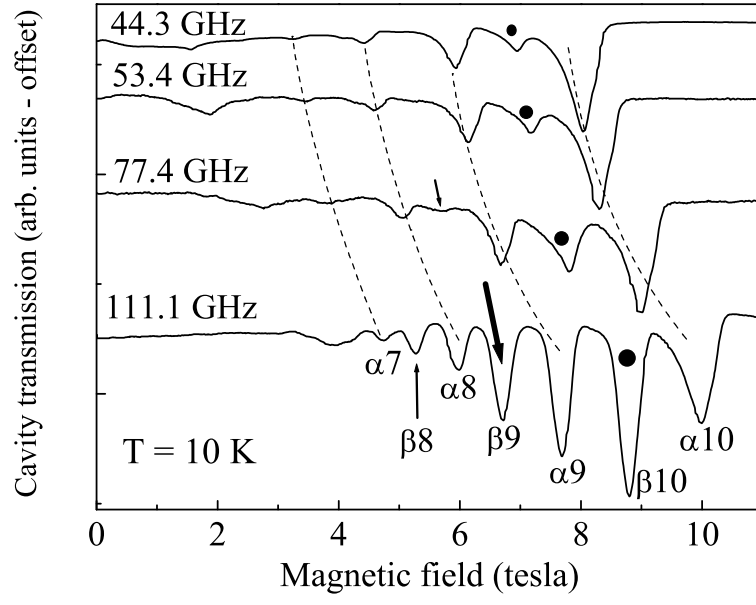
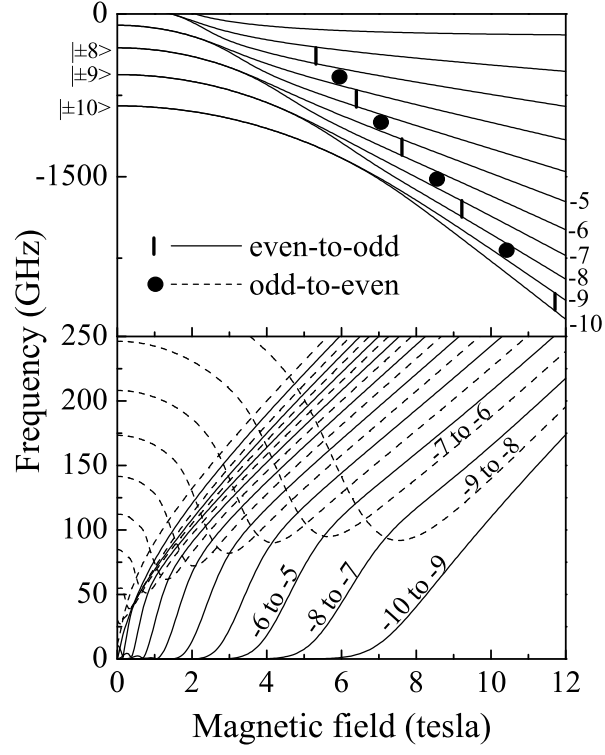
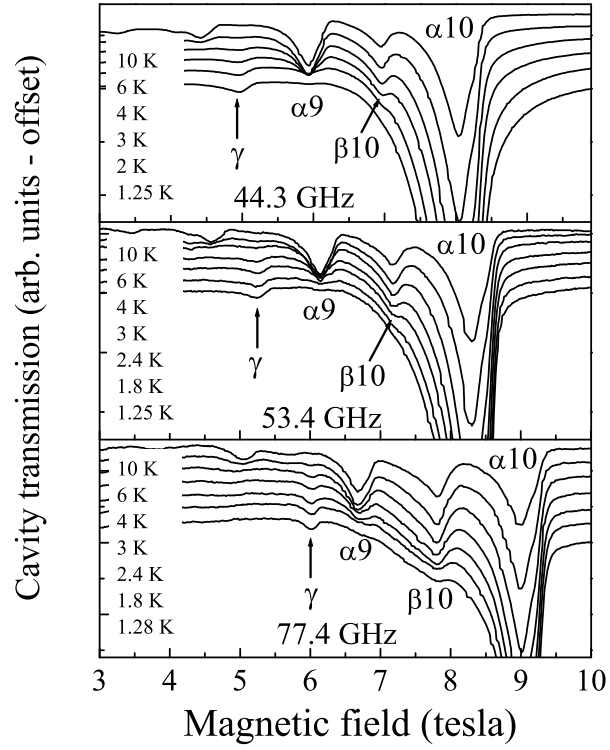
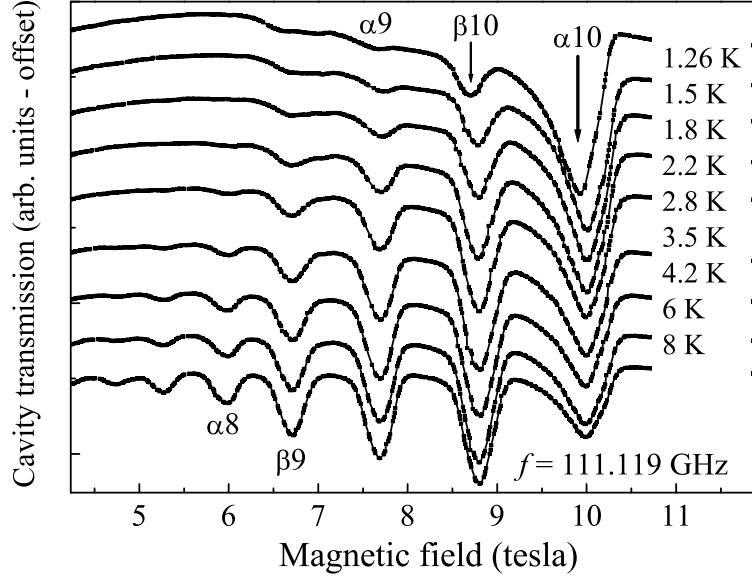
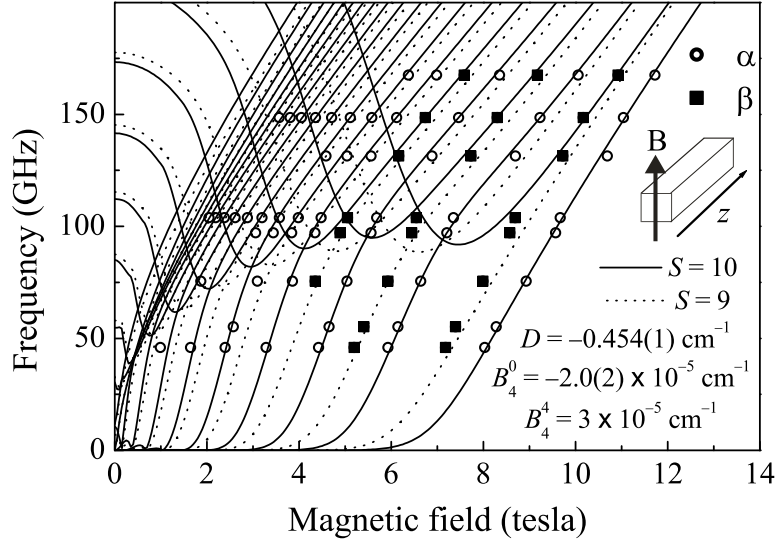


FIG. 1: S. Hill *et al.*

FIG. 2: S. Hill *et al.*FIG. 3: S. Hill *et al.*

FIG. 4: S. Hill *et al.*FIG. 5: S. Hill *et al.*